Journal of Magnetic Resonance 225 (2012) 115–119

Contents lists available at SciVerse ScienceDirect

Journal of Magnetic Resonance

journal homepage: www.elsevier.com/locate/jmr

Communication

HyperSPASM NMR: A new approach to single-shot 2D correlations on DNP-enhanced samples

Kevin J. Donovan, Lucio Frydman *

Chemical Physics Department, Weizmann Institute of Science, 76100 Rehovot, Israel

ARTICLE INFO

Article history:
Received 29 August 2012
Revised 10 October 2012
Available online 29 October 2012

Keywords:
2D NMR
Dissolution DNP
Hyperpolarization
Heteronuclear correlations
Ultrafast NMR

ABSTRACT

Dissolution DNP experiments are limited to a single or at most a few scans, before the non-Boltzmann magnetization has been consumed. This makes it impractical to record 2D NMR data by conventional, t_1-incremented schemes. Here a new approach termed *HyperSPASM* to establish 2D heteronuclear correlations in a single scan is reported, aimed at dealing with this kind of challenge. The *HyperSPASM* experiment relies on imposing an amplitude-modulation of the data by a single Δt_1 indirect-domain evolution time, and subsequently monitoring the imparted encoding on separate echo and anti-echo pathway signals within a single continuous acquisition. This is implemented via the use of alternating, switching, coherence selection gradients. As a result of these manipulations the phase imparted by a heteronucleus over its indirect domain evolution can be accurately extracted, and 2D data unambiguously reconstructed with a single-shot excitation. The nature of this sequence makes the resulting experiment particularly well suited for collecting indirectly-detected HSQC data on hyperpolarized samples. The potential of the ensuing *HyperSPASM* method is exemplified with natural-abundance hyperpolarized correlations on model systems.

1. Introduction

By establishing unambiguous connectivity, two-dimensional (2D) NMR conveys unique information about a molecule's structure and dynamics at an atomic resolution. 2D NMR correlations typically require a full sampling of two time-domains according to Nyquist criteria [1,2]; as one of these domains involves a t_1 delay within a pulse sequence, this necessitates multiple repetitions and extended experimental timescales. Numerous proposals have emerged to reduce these acquisition times, including sparse sampling techniques [3–8] and other non-Fourier methods [9,10]. Although facilitating higher-throughput and faster high-D NMR spectroscopy, these approaches still do not eliminate the necessity for collecting multiple scans. Such requirement for multiple acquisitions complicates the prospects of combining 2D NMR with dissolution Dynamic Nuclear Polarization (DNP) [11–13]. Dissolution DNP is a promising emerging technique [14], whereby a hyperpolarized spin state is created in a cryogenic solid and then suddenly melted so as to exploit it for a dramatic sensitivity enhancement in solution NMR or MRI. This hyperpolarization, however, decays with the longitudinal relaxation time T_1, and it cannot be preserved at the level of constancy normally demanded by conventional 2D NMR acquisitions. By contrast, ultrafast 2D techniques that rely on spatio-temporal encodings to monitor the indirect-domain evolution [15,16], have been shown capable of making full use of this hyperpolarization [17–19]. While spatio-temporal methods can deliver 2D NMR spectra in a single scan without *a priori* knowledge, they face a number of technical limitations. Most prominent among these is the signal-to-noise penalty associated with having to acquire data along two spectral dimensions simultaneously. Given that the per-scan noise in these methods increases as the root of the number of elements along F_1, this may be particularly onerous when this axis involves nuclei that, like ^{13}C, are associated with sharp resonances spanning a wide frequency range. This Communication presents an alternative for acquiring single-shot 2D hyperpolarized data, Single-Point Amplitude-Separated Multi-dimensional (SPASM) NMR, that is specifically designed to bypass these limitations and to maximize the sensitivity enhancement provided by dissolution DNP.

The SPASM approach draws from two previous developments in the area of accelerated multidimensional acquisitions. One of these is single-point evaluation of the evolution dimension (SPEED) spectroscopy [20], where correlations among resolved chemical sites are sought from the phase shift imparted on F_2 peaks when 2D data are acquired for a known Δt_1 t_1-value. This information can be exploited owing to the defined distortions that this F_1 evolution will introduce on the $I(F_2)$ shape of peaks along the direct domain, as given by

$$S(t_1, F_2) \approx exp(2\pi i F_1 \Delta t_1) \cdot I(F_2) \cdot exp[2\pi i(\phi_o + F_2\phi_1)] \quad (1)$$

* Corresponding author. Fax: +972 8 9344123.
E-mail address: lucio.frydman@weizmann.ac.il (L. Frydman).

1090-7807/$ - see front matter © 2012 Elsevier Inc. All rights reserved.
http://dx.doi.org/10.1016/j.jmr.2012.10.006

Although well-defined, notice that an ambiguity remains in this determination owing to the last term in Eq. (1), involving the constant and linear phase distortions ϕ_o, ϕ_1 of common occurrence in 1D NMR. In order to remove these unknowns while preserving the experiment's single-shot character, we propose to incorporate onto it a second development from the 2D NMR literature: the switched acquisition time (SWAT) experiment [21]. Originally proposed for the simultaneous collection of N- and P-type 2D COSY data, this method operates by imposing an initial coherence-selection encoding gradient during t_1, and subsequently interleaving coherence-selective decoding gradients between sampled points in t_2. Moreover, following the decoding of the first t_2-point, each of these coherence decoding gradients is applied with a strength corresponding to twice the action of the initial coherence encoding; this allows one to "jump" from echo- to anti-echo acquisition FIDs between consecutively sampled data points.

Combining the principles underlying these two techniques, SPEED and SWAT, along the guidelines shown in Fig. 1, allows one to resolve the indirect-dimension ambiguity remaining in Eq. (1) within a single-scan sequence. Indeed, even if constrained to a single t_1 value Δt_1, the phase distortions in the resulting acquisition can be summarized as

$$\begin{aligned} S_N(\Delta t_1, F_2) &\approx exp(-2\pi i F_1 \Delta t_1) \cdot I(F_2) \cdot exp[2\pi i(\phi_o + F_2\phi_1)] \\ S_P(\Delta t_1, F_2) &\approx exp(+2\pi i F_1 \Delta t_1) \cdot I(F_2) \cdot exp[2\pi i(\phi_o + F_2\phi_1 \Delta t_{SWAT})] \end{aligned} \quad (2)$$

where Δt_{SWAT} is the delay between N and P's initial acquisition time. Given that this delay is known, the difference required by each F_2-peak of N- and P-spectra for achieving its correct phasing:

$$\begin{aligned} \Delta\phi(F_2) &= \tan^{-1}[im(S_p)/re(S_p)] - \tan^{-1}[im(S_N)/re(S_N)] \\ &= 4\pi F_1 \Delta t_1 + F_2 \Delta t_{SWAT} \end{aligned} \quad (3)$$

can ascertain the F_1 offset to be correlated with this peak – all while remaining in a single-shot acquisition mode and without incurring the sensitivity penalties of space-encoded ultrafast NMR.

2. Experimental methods

The usefulness of HyperSPASM was explored within the context of *ex situ* DNP. Such dissolution DNP experiments are well suited for heteronuclear correlations whereby the slowly-relaxing ^{13}C nuclei are hyperpolarized, and then monitored indirectly in correlation with J-coupled protons having a higher detection sensitivity. The HyperSPASM experiment thus assayed (Fig. 1) resembles a reversal of the traditional HETCOR sequence [23]. Notice as well that a small-tip-angle ^{13}C "twilight" 1D acquisition is collected as complement to SPASM, and is meant to provide an unambiguous accounting of all the ^{13}C positions expected along the F_1 domain.

Samples were hyperpolarized in an Oxford Hypersense polarizer (Tubney Woods, UK) for 5 h (pyridine) and 3.25 h (indazole). Pyridine was hyperpolarized by BDPA radicals at ≈40 mM with an equal volume of d_6-DMSO. Indazole was hyperpolarized in a 1:1 solution of d_6-DMSO/sulfolane with 40 mM BDPA [24]. Approximately 4 mL of methanol-d_4 were used to dissolve both samples. The encoding gradient following the indirect evolution delay (Δt_1) was set to 20 G/cm, which then determined the decode gradient immediately before SWAT acquisition by the ratio (γ_C/γ_H) to be approximately 5 G/cm and the SWAT acquisition gradients to be approximately 10 G/cm. All of the aforementioned coherence selection gradients were applied for a length of 200 μs. The y and z gradients used in the GBIRD element had amplitude 30 G/cm and a length of 400 μs. The HyperSPASM experiment shown in Fig. 1 was repeated for two transients (where the ^{13}C twilight acquisition was collected only on the first transient) to achieve complete suppression of the ^{12}C-bonded protons, where the phase of the 90-degree carbon pulse preceding Δt_1 was inverted and the resulting signals were subtracted by alternating the receiver phase. As an additional step to achieve background signal suppression, the correlation sequence was preceded by a 90-degree pulse on the ^1H channel followed by an approximately 13.3 G/cm gradient on the PFG X-axis channel for a duration of 1 ms, to dephase any initial ^1H magnetization such that it would not contribute to the detected signal.

3. Results

To better visualize the workings of the resulting scheme, Fig. 2 illustrates SPASM's operation for a heteronuclear correlation in a model compound. Notice the phase-wrapping that naturally occurs as the F_1 offset exceeds $\pm 0.5/\Delta t_1$; it follows from plots of this type that Δt_1 not only imposes this frequency range but also ΔF_1's resolution limit. According to repetitive SPASM measurements and their ensuing P/N-phasing, we estimate this random uncertainty at ca. $0.015/\Delta t_1$.

Fig. 3 illustrates the ensuing results for pyridine and for indazole. Notice that with a suitable placing of the RF channel's offsets in the center of the corresponding spectra, the experiment had no difficulties in correlating each $^1H/^{13}C$ coupled pair while monitoring free evolution data – this, despite the latter shifts spanning nearly 3 kHz in F_1. The single-shot correlation shows excellent agreement with HSQC [25] data acquired and processed [26] in a conventional manner. The ^{13}C "twilight" 1D acquisition further

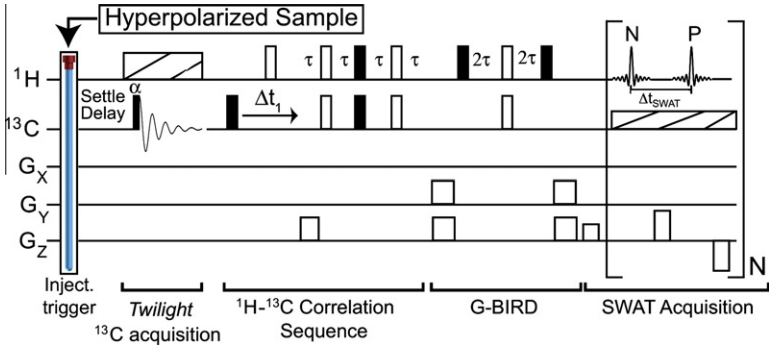

Fig. 1. HyperSPASM pulse sequence for establishing single-shot 2D heteronuclear correlations on DNP-enhanced samples. A single-t_1 (Δt_1) 2D heteronuclear sequence – with full and open rectangles representing $\pi/2$ and π pulses respectively, dashed rectangles denoting broadband decoupling, and $\tau = 1/(4J_{CH})$ set by one-bond heteronuclear couplings – establishes the ^{13}C–^1H correlations. The absolute phase evolution imparted by Δt_1 is unraveled by the independent, single-shot monitoring of echo and anti-echo (N,P) modulations as aided by pulsed G_Z gradients. The sequence includes a G_X, G_Y-BIRD element [22] to suppress background signals from ^{12}C bonded protons, and thereby enable the acquisition of ^{13}C-decoupled direct domain line shapes that can be independently and reliably phased to pure absorption. An initial twilight $\{^1H\}^{13}C$ spectrum is also acquired using a low flip-angle pulse before the acquisition, as an aid to remove potential folding artifacts in F_1.

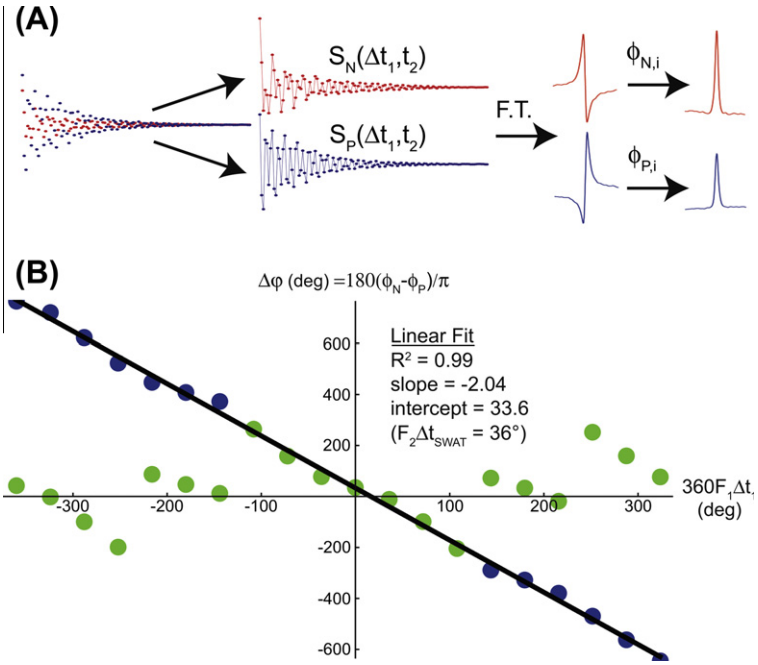

Fig. 2. Experimental demonstration of SPASM's ability to measure indirect-domain evolution frequencies, illustrated for a model Chloroform case whose ^{13}C offset was systematically shifted over 2 kHz in 100 Hz steps for a fixed indirect evolution delay Δt_1 = 1 ms. (A) Post-acquisition processing involves separating the experimental data into alternating points corresponding to N (echo) and P (anti-echo) FIDs. Once individually Fourier transformed and phased to yield purely-absorptive 1D spectra, each peak leads to the phase parameters $\phi_{N,i}$ and $\phi_{P,i}$, from which the indirect frequency can be determined (Eq. (2)). (B) Phase difference exhibited by $CHCl_3$'s sole ^1H resonance when acted upon by the SP-SWAT sequence as a function of an artificially-varying indirect frequency offset F_1. Green data points illustrate the periodic phase wrapping arising from the limits on a measurable phase difference $\Delta\phi = \phi_N - \phi_P$; phase-unwrapping yields the blue points, in excellent fit with the prediction of Eq. (3). (For interpretation of the references to color in this figure legend, the reader is referred to the web version of this article.)

validates the genuine frequencies of all indirect-domain peaks from SPASM data. Still, it is interesting to note certain systematic deviations between the positions of the ^{13}C peaks observed by this pre-acquisition scan and the SPASM predictions for all peaks that were analyzed. We ascribe these deviations to minor timing errors in the implementation of the gradient's and pulse's waveforms, whose exact value was unknown and therefore ignored in the F_1-domain estimations.

To further assess the experimental sensitivity benefit incurred from the dissolution DNP process, the results obtained with HyperSPASM were compared with results obtained on the same sample after spins have returned to thermal equilibrium. Both experiments used the pulse sequence in Fig. 1 (in the thermal case, without the twilight ^{13}C acquisition), and the latter was repeated for 512 transients. Fig. 4 presents this control, and reveals that *ca.* 670× and 120× average enhancements characterize the Echo and Anti-echo spectral acquisitions arising from pyridine and indazole dissolutions, respectively. When factoring in the additional γ_H/γ_C sensitivity afforded by these ^1H-detected experiments it follows that HyperSPASM imparts very modest sensitivity penalties over the conventionally detected 1D DNP-enhanced ^{13}C experiment – despite the more complex nature of the used pulse sequence and the 2D correlated information arising thereof. Also interesting to note is the 180° phase shift differences characterizing all peaks in the hyperpolarized vs the thermal spectra illustrated in Fig. 4; given the identical pulse sequences that were utilized to collect these two data sets, we ascribe this difference to the opposing states of ^{13}C polarization that characterized the initial states in these experiments.

4. Discussion and conclusions

This study introduced a new approach to establish 2D NMR correlations, whereby single-delay phase distortions can be translated into F_1 shifts. This can be attained in a single scan by the simultaneous acquisition of the echo and anti-echo sets arising from amplitude-modulated data involving a single Δt_1 time. The experiment is unequivocal and accurate, providing a convenient platform for extracting DNP-enhanced 2D correlations. Being free from the need to fully sample two domains in a single scan, the acquired spectra also promise remarkable signal-to-noise improvements vis-à-vis ultrafast 2D NMR. This technique could thereby be advantageously extended beyond its integration of DNP and into other kinds of time-pressed experiments, like the monitoring of real time chemical processes at seconds or sub-second timescales [27]. Despite all these promises, this technology still faces a number of basic limitations related to the extraction of frequencies from a single time point. One of these relates to folding/phase-wrapping ambiguities, which can usually be alleviated by adding the aforementioned 1D "twilight" measurement. Another limitation stems from the inter-relation between the spectral width that can be characterized in F_1, and the accuracy of these characterizations – both of which end up defined by the same parameter Δt_1. Arguably, however, the most constraining limitation stems from the requirement that all peaks of interest be resolved along the direct dimension. In effect, should one F_2 peak be correlated to multiple F_1 sites, phasing such resonance into a reliable purely-absorptive line shape from which a definite F_1 offset value could be read from the ϕ_N and ϕ_P parameters, does not appear feasible. For large complex molecules like proteins, or for multi-site homonuclear correlation experiments such as TOCSY, the sequence in Fig. 1 would seem of little use. The use of additional manipulations, however, could help alleviate this problem. One could envision, for instance, incorporating additional coherence-selecting gradients encoding supplementary Δt_1 values, from which the ensuing ambiguities could be resolved. Research on how to solve this matter and exploring its applications, is currently in progress.

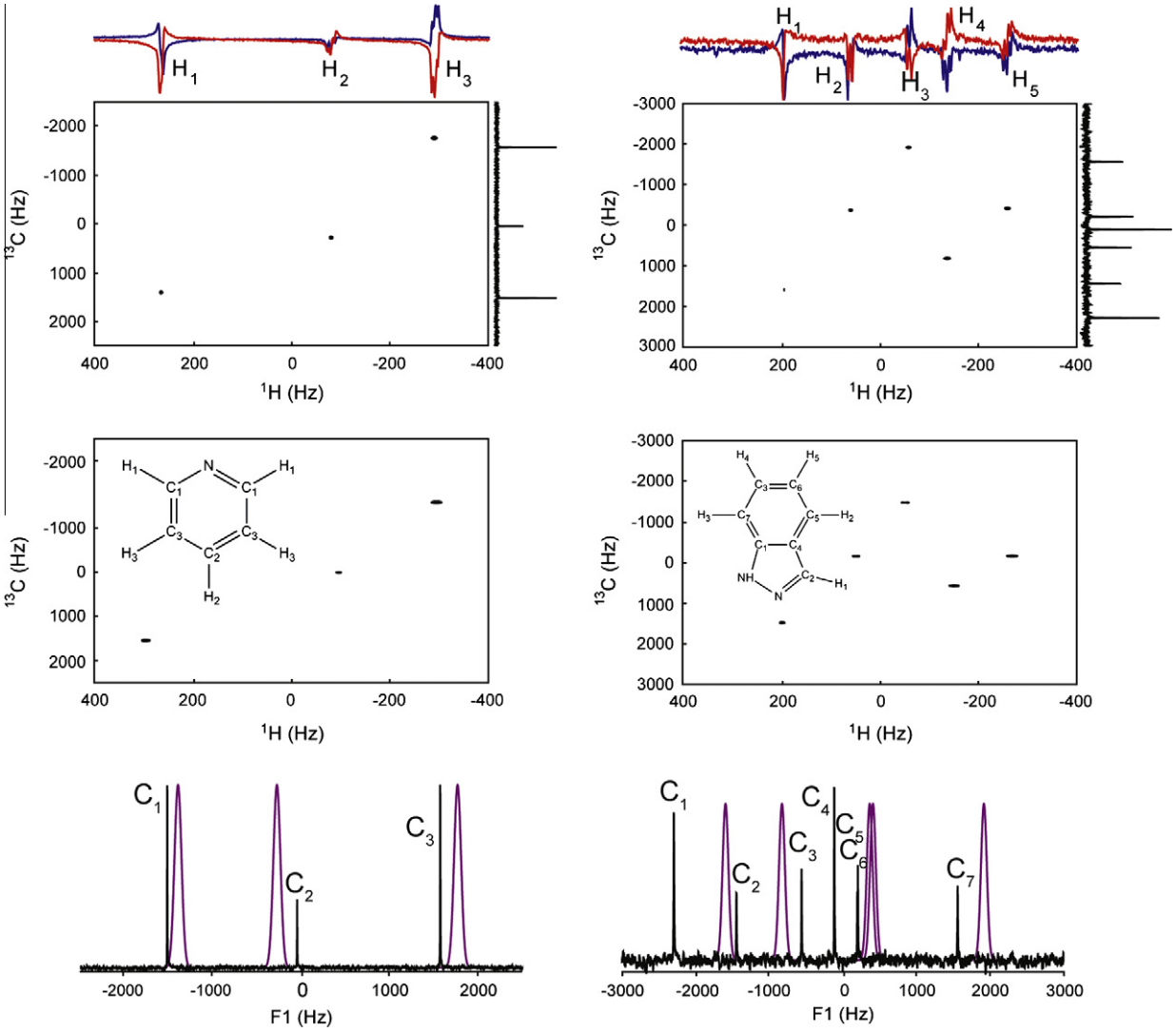

Fig. 3. HyperSPASM correlations established for natural-abundance pyridine (left) and indazole (right). The 2D correlations generated by the pulse sequence (upper panels) arise from phasing the illustrated 1D traces – *N*/echo spectrum in red, *P*/anti-echo spectrum in blue. Each of these was collected using the sequence in Fig. 1, $N = 256$ acquisition loops, $\Delta t_1 = 150$ μs, and two phase-cycled transients for an optimal suppression of the ^{12}C-bonded protons (important to retrieve reliable phased data). Shown in the lower 2D panels are conventional HSQC spectra acquired with 256 t_1 increments. HyperSPASM data were acquired at sample concentrations of ≈3 mM for pyridine and 20 mM for indazole, the thermal HSQCs stem from concentrated (approximately 25% pyridine, 1 M indazole) samples. The 1D spectra (bottom) compare the predicted F_1 peak locations calculated from Eq. (3) (violet) against the experimental DNP-enhanced *twilight* ^{13}C data (black); widths in the calculated peaks reflect the phasing uncertainty, translated into Hz. (For interpretation of the references to colour in this figure legend, the reader is referred to the web version of this article.)

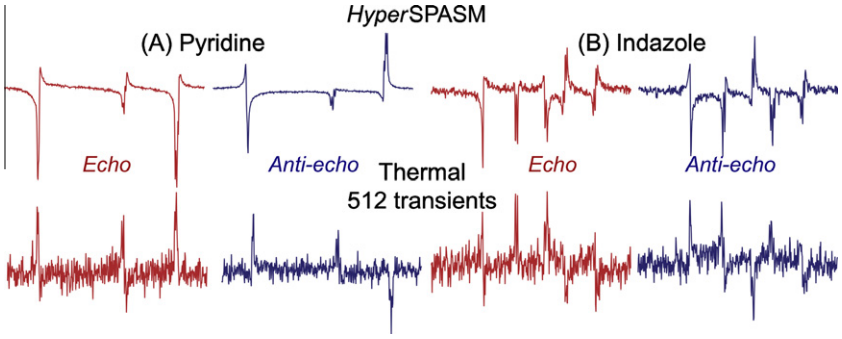

Fig. 4. Comparing SPASM's sequence performance on DNP-enhanced samples (one post-twilight scan – top) *vs* the same sequence executed after spins have returned to their thermal equilibrium (bottom), for both pyridine (A) and indazole (B). We ascribe the ≈180° phase difference between hyperpolarized and thermal spectra to the differing initial conditions of the starting ^{13}C polarization.

Acknowledgments

The authors thank L. Casabianca, C. Bretschneider and T. Harris for assistance in the DNP experiments, and to E. Kupce for programming insight. Financial support from Agilent Technologies (Research Gift #2305), ERC Advanced Grant #246754, EU'S BioNMR Grant #261863, and the generosity of the Perlman Family Foundation, are also acknowledged.

References

[1] J. Jeener (Ed.), Lecture Presented at Ampere International Summer School II, Basko Polje, Yugoslavia, 1971.
[2] R.R. Ernst, G. Bodenhausen, A. Wokaun (Eds.), Principles of Nuclear Magnetic Resonance in One and Two Dimensions, Oxford University Press, 1987.
[3] J.C. Hoch, A.C. Stern (Eds.), NMR Data Processing, John Wiley and Sons, Inc. 1996.
[4] J. Chen, A.A. De Angelis, V.A. Mandelshtam, A.J. Shaka, Progress on the two-dimensional filter diagonalization mehod. An efficient doubling scheme for two-dimensional constant-time NMR, J. Magn. Reson. 162 (2003) 74–89.
[5] E. Kupce, R. Freeman, Projection-reconstruction technique for speeding up multidimensional NMR spectroscopy, J. Am. Chem. Soc. 126 (2004) 6429–6440.
[6] S. Hiller, F. Fiorito, K. Wuthrich, G. Wider, Automated Projection Spectroscopy (APSY), Proc. Natl. Acad. Sci. USA 102 (2005) 10876–10881.
[7] K. Kazimierczuk, J. Stanek, A. Zawadzka-Kazimierczuk, W. Koźmiński, Random sampling in multidimensional NMR spectroscopy, Prog. Nucl. Magn. Reson. Spectrosc. 57 (2010) 420–434.
[8] V.Y. Orekhov, V.A. Jaravine, Analysis of non-uniformly sampled spectra with multi-dimensional decomposition, Prog. Nucl. Magn. Reson. Spectrosc. 59 (2011) 271–292.
[9] E. Kupce, R. Freeman, Two-dimensional Hadamard spectroscopy, J. Mag. Reson. 162 (2003) 300–310.
[10] S. Kim, T. Szyperski, GFT NMR, a new approach to rapidly obtain precise high-dimensional NMR spectral information, J. Am. Chem. Soc. 125 (2003) 1385–1393.
[11] S. Bowen, H. Zeng, C. Hilty, Chemical shift correlations from hyperpolarized NMR by off-resonance decoupling, Anal. Chem. 80 (2008) 5794–5798.
[12] C. Ludwig, I. Marin-Montesinos, M.G. Saunders, U.L. Gunther, Optimizing the polarization matrix for *ex situ* dynamic nuclear polarization, J. Am. Chem. Soc. 132 (2010) 2508–2509.
[13] H. Zeng, S. Bowen, C. Hilty, Sequentially acquired two-dimensional NMR spectra from hyperpolarized sample, J. Magn. Reson. 199 (2009) 159–165.
[14] J.H. Ardenkjær-Larsen, B. Fridlund, A. Gram, G. Hansson, L. Hansson, M.H. Lerche, R. Servin, M. Thaning, K. Golman, Increase in signal-to-noise ratio of >10,000 times in liquid-state NMR, Proc. Natl. Acad. Sci. USA 100 (2003) 10158–10163 (Also, see the themed issue on Dynamic Nuclear Polarization, Phys. Chem. Chem. Phys. (2010), 12).
[15] L. Frydman, T. Scherf, A. Lupulescu, The acquisition of multidimensional NMR spectra within a single scan, Proc. Natl. Acad. Sci. USA 99 (2002) 15858–15862.
[16] M. Mishkovsky, L. Frydman, Principles and progress in ultrafast multidimensional nuclear magnetic resonance, Annu. Rev. Phys. Chem. 60 (2009) 429–448.
[17] L. Frydman, D. Blazina, Ultrafast two-dimensional nuclear magnetic resonance spectroscopy of hyperpolarized solutions, Nat. Phys. 3 (2007) 415–419.
[18] M. Mishkovsky, L. Frydman, Progress in hyperpolarized ultrafast 2D NMR spectroscopy, ChemPhysChem 9 (2008) 2340–2348.
[19] P. Giraudeau, Y. Shrot, L. Frydman, Multiple ultrafast, broadband 2D NMR spectra of hyperpolarized natural products, J. Am. Chem. Soc. 131 (2009) 13902–13903.
[20] E. Kupce, R. Freeman, SPEED: single-point evaluation of the evolution dimension, Magn. Reson. Chem. 45 (2007) 711–713.
[21] R.E. Hurd, B.K. John, H.D. Plant, Novel method for detection of pure-phase, double-absorption lineshapes in gradient-enhanced spectroscopy, J. Magn. Reson. 93 (1991) 666–670.
[22] C. Emetarom, T.L. Hwang, G. Mackin, A.J. Shaka, Isotope editing of NMR spectra. Excitation sculpting using BIRD pulses, J. Magn. Reson. 115 (1995) 137–140.
[23] R. Freeman, G.A. Morris, Experimental chemical shift correlation maps in nuclear magnetic resonance spectroscopy, J. Chem. Soc. Chem. Comm. (1978) 684–686.
[24] L. Lumata, S.J. Ratnakar, R. Jindal, M. Merritt, A. Comment, C. Malloy, A.D. Sherry, Z. Kovacs, BDPA: an efficient polarizing agent for fast dissolution dynamic nuclear polarization NMR spectroscopy, Chem. Eur. J. 17 (2011) 10825–10827.
[25] G. Bodenhausen, D.J. Ruben, Natural abundance nitrogen-15 NMR by enhanced heteronuclear spectroscopy, Chem. Phys. Lett. 69 (1980) 185–189.
[26] F. Delaglio, S. Grzesiek, G. Vuister, G. Zhu, J. Pfeifer, A. Bax, NMRPipe: A multidimensional spectral processing system based on UNIX pipes, J. Biomol. NMR. 6 (1995) 277–293.
[27] M. Gal, M. Mishkovsky, L. Frydman, Real-time monitoring of chemical transformations by ultrafast 2D NMR spectroscopy, J. Am. Chem. Soc. 128 (2006) 951–956.